Supporting Information

Correlating Phase Behaviour with Photophysical Properties in Mixed-Cation Mixed-Halide Perovskite Thin Films

*Claire Greenland, Adam Shnier, Sai K. Rajendran, Joel A. Smith, Onkar Game, Daniel Wamwangi, Graham A. Turnbull, Ifor D.W. Samuel, David G. Billing, David G. Lidzey**

All data has been collected from a solution-processed thin film of $(FAPbI_3)_{0.85}(MAPbBr_3)_{0.15}$ fabricated as described in Section 4 of the main paper, unless otherwise stated.

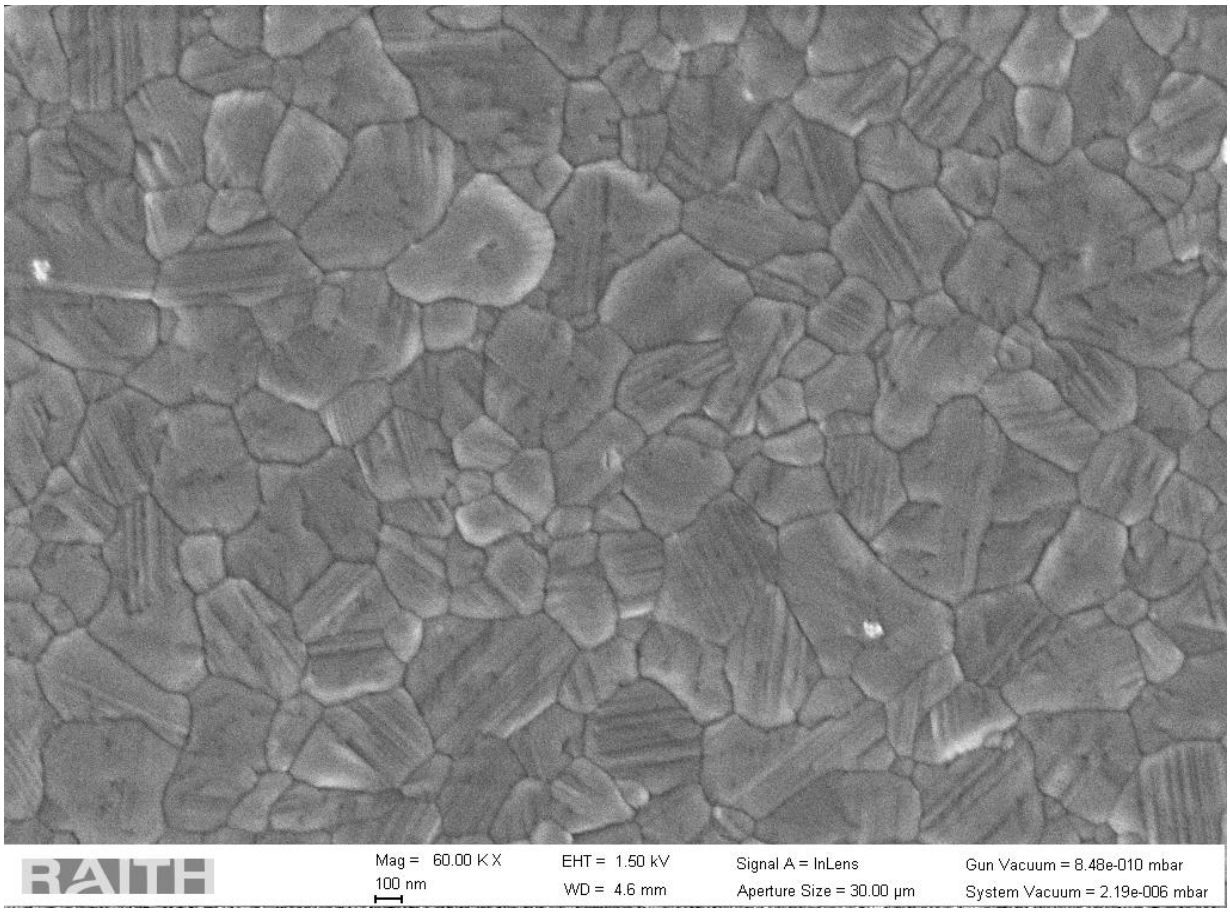

Figure S1: Scanning electron microscopy image of the $(FAPbI_3)_{0.85}(MAPbBr_3)_{0.15}$ sample surface at 60,000x magnification.

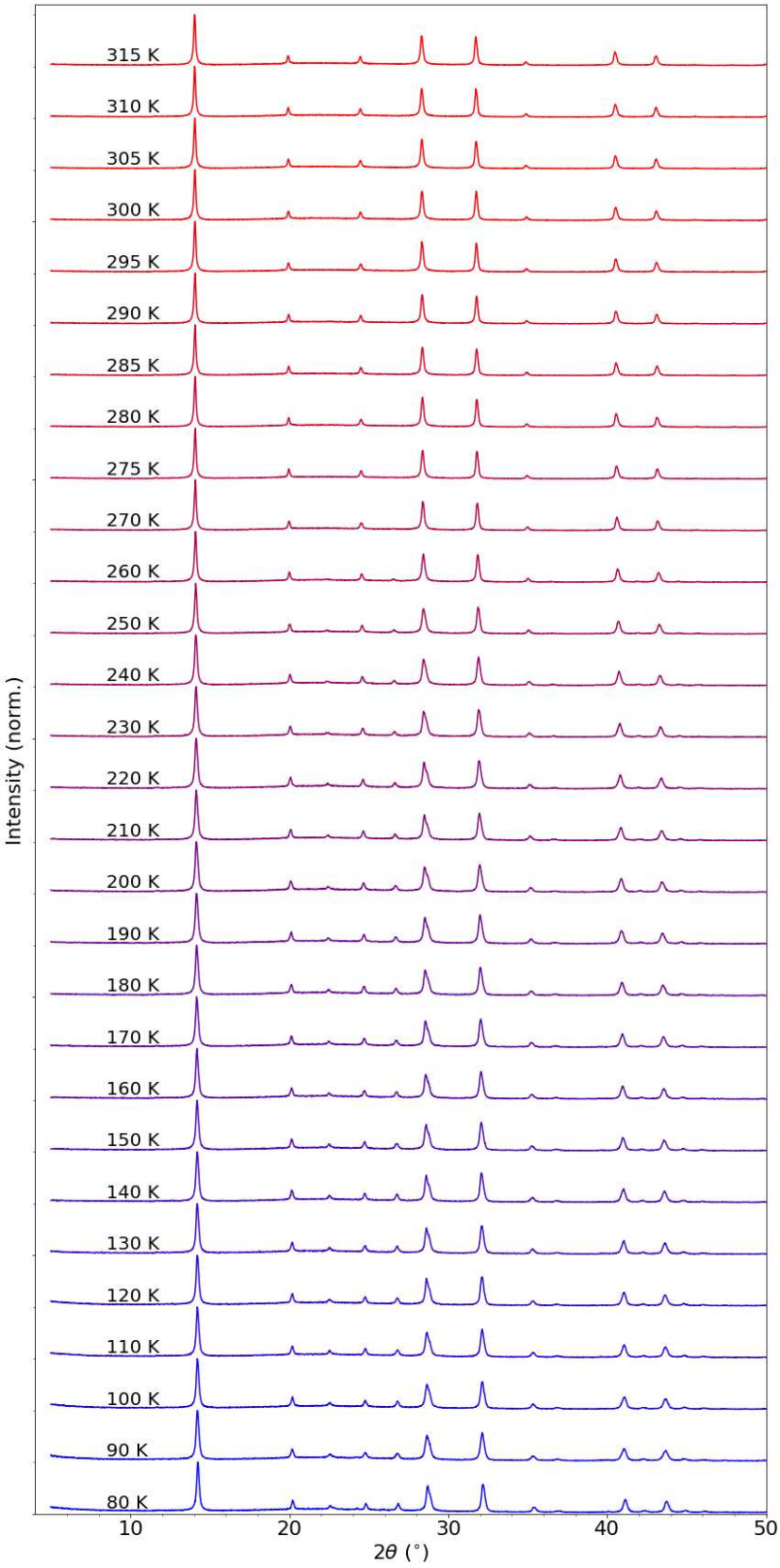

Figure S2a: Full PXRD scattering patterns on powdered films for all temperatures on cooling from 315 K to 80 K.

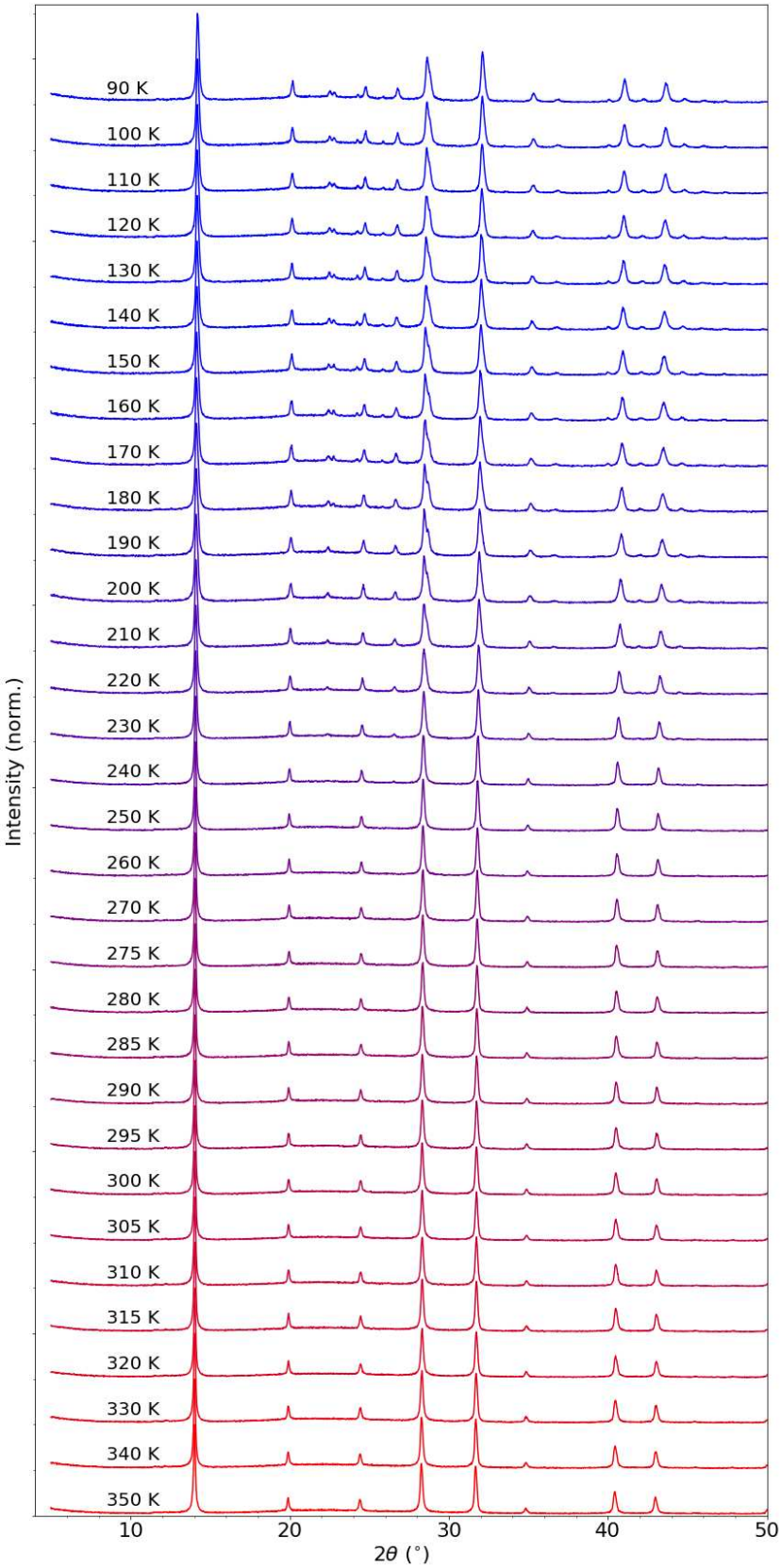

Figure S2b: Full PXRD patterns on powdered films for all temperatures during heating from 90 K to 350 K.

Supplementary Note 1: Structural Modelling

1.1 Pearson VII fits

To extract some minimally convoluted information a selection of peaks were modelled sequentially using a Pearson VII analytical peak fitting with TOPAS V5.0 across the VT-PXRD data. From this we observe a broadening in the distribution of peak position changes above 270 K. Considering the peak positions are normalised by their maximum, this is consistent with the relative elongation of an axis during the α to β phase transition. Between 210 and 270 K during heating the FWHM of many peaks broadens with decreasing temperature. The equivalent is observed during cooling only in a narrower range between 230 and 270 K, on cooling the (111) and (211) peaks experience no change of the same magnitude. While on heating the (111) peak is narrower at 315 K and above. Much of the broadening of peaks is attributed crystallographic planes becoming inequivalent as the symmetry of the unit cell changes leading the splitting of peaks such as where 100, 010, and 001 become inequivalent on cooling. A δ phase is suspected at 80 K where there is a sudden increase in the lattice parameters as seen in Figure 3**(a)** and **(b)** by the shift of the peaks to higher angles.

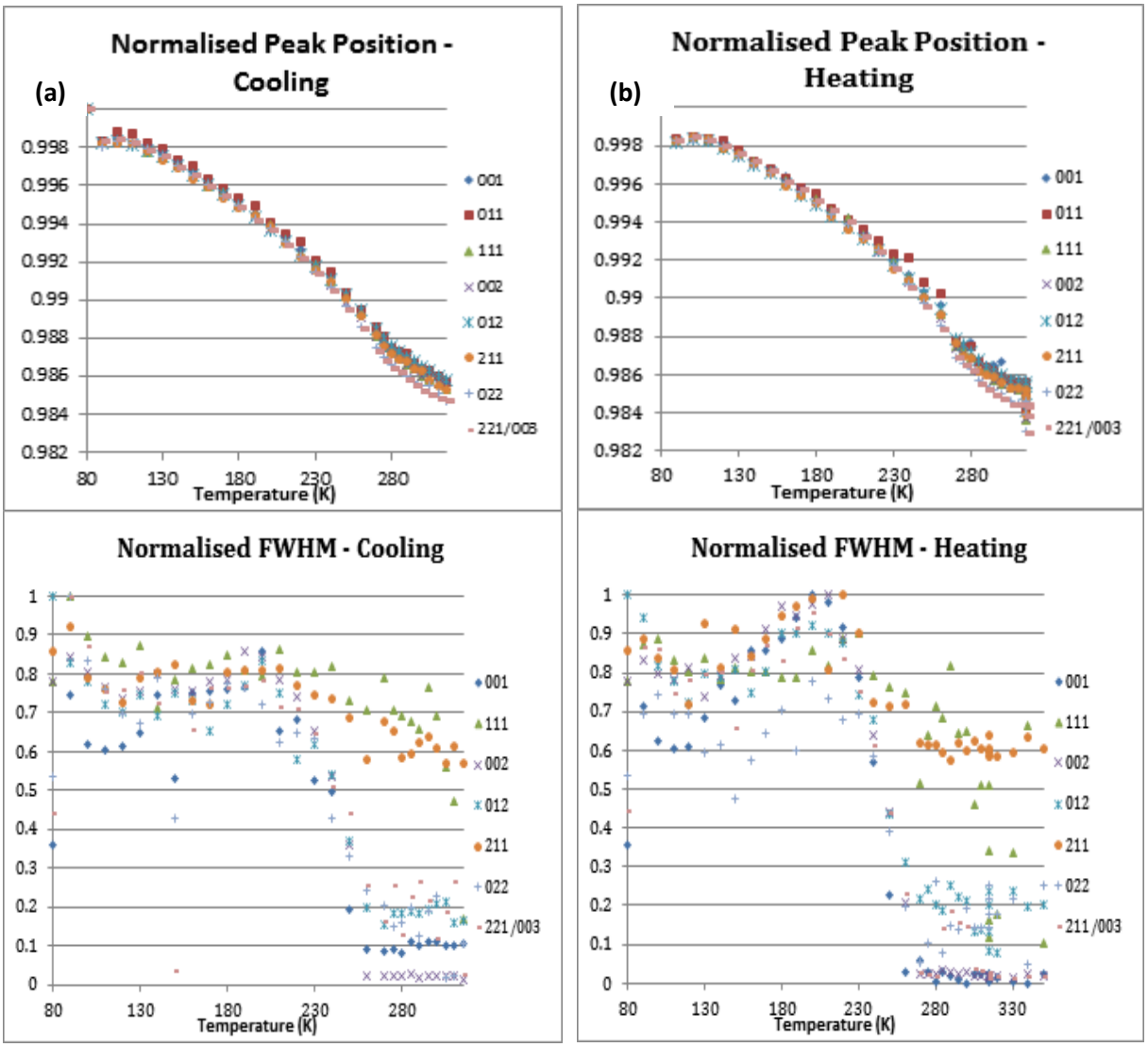

Figure S3: PXRD peak parameters extracted from the Pearson VII fits. **(a)** Normalised peak positions as a function of temperature on cooling. **(b)** Normalised peak positions as a function of temperature on heating. **(c)** Normalised FWHM of key peaks as a function of temperature on cooling. **(d)** Normalised FWHM of key peaks as a function of temperature on heating.

1.2 Rietveld refinements

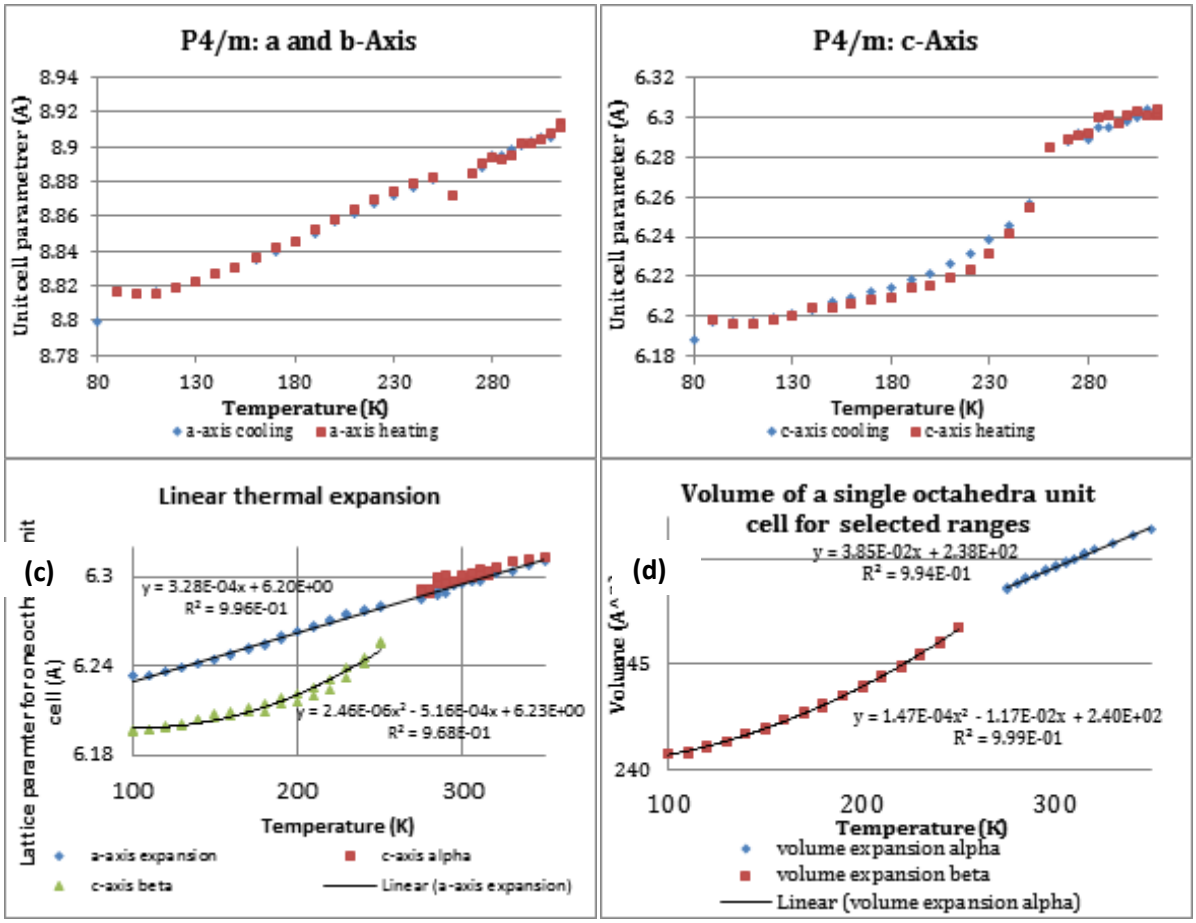

Figure S4: PXRD peak parameters extracted from the Rietveld structure refinements. **(a)** Evolution of the *a*/*b*-axis parameter with temperature, assuming a *P4/m* space group. **(b)** Evolution of the *c*-axis parameter with temperature, assuming a *P4/m* space group. **(c)** Volumetric thermal expansion of the octahedral unit cell for the α and β phases. **(d)** Linear thermal expansion of the a- and *c*-axis parameters of the unit cell for the α and β phases.

.

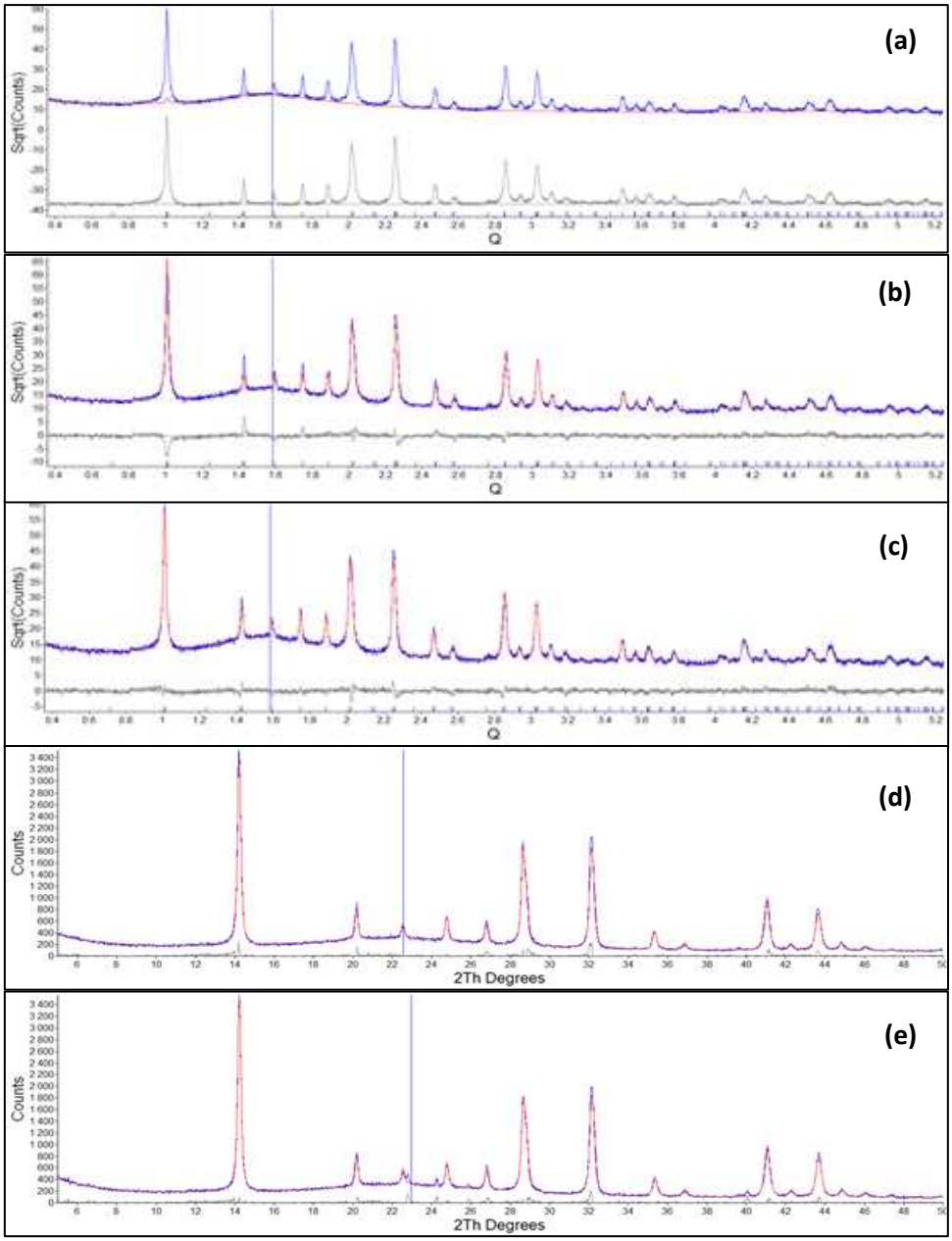

Figure S5: (a) Blue line: raw data taken at 150 K on cooling of the sample. Red line: calculated fit from the Rietveld structure refinements. Grey line: difference between the raw data and calculated fit. **(b)** Blue line: raw data taken at 150 K on cooling of the sample. Red line: contribution of the FA cation to the calculated fit from the Rietveld structure refinements. Grey line: difference between the raw data and the FA contribution. **(c)** Blue line: raw data taken at 150 K on cooling of the sample. Red line: contribution of the PbX anion to the calculated fit from the Rietveld structure refinements. Grey line: difference between the raw data and the PbX contribution. **(d)** Blue line: raw data taken at 120 K on cooling of the sample. Red line: calculated fit from the Rietvield refinement. **(e)** Blue line: raw data taken at 100 K on re-heating of the sample. Red line: calculated fit from the Rietvield refinement. The Pb cations are positioned on the (001) plane of the unit cell while the FA cations are roughly on the (002) plane. The interaction between the cation then results in destructive interference when scattering from the 001 and near equivalent planes as seen by the negative counts in the difference curve for the contribution of PbX. In Figure 5**(d)** and **(e)** we see unidentified extra peaks on the heating cycle that are not present during the cooling of the perovskite. These peaks disappear between 210 and 220 K.

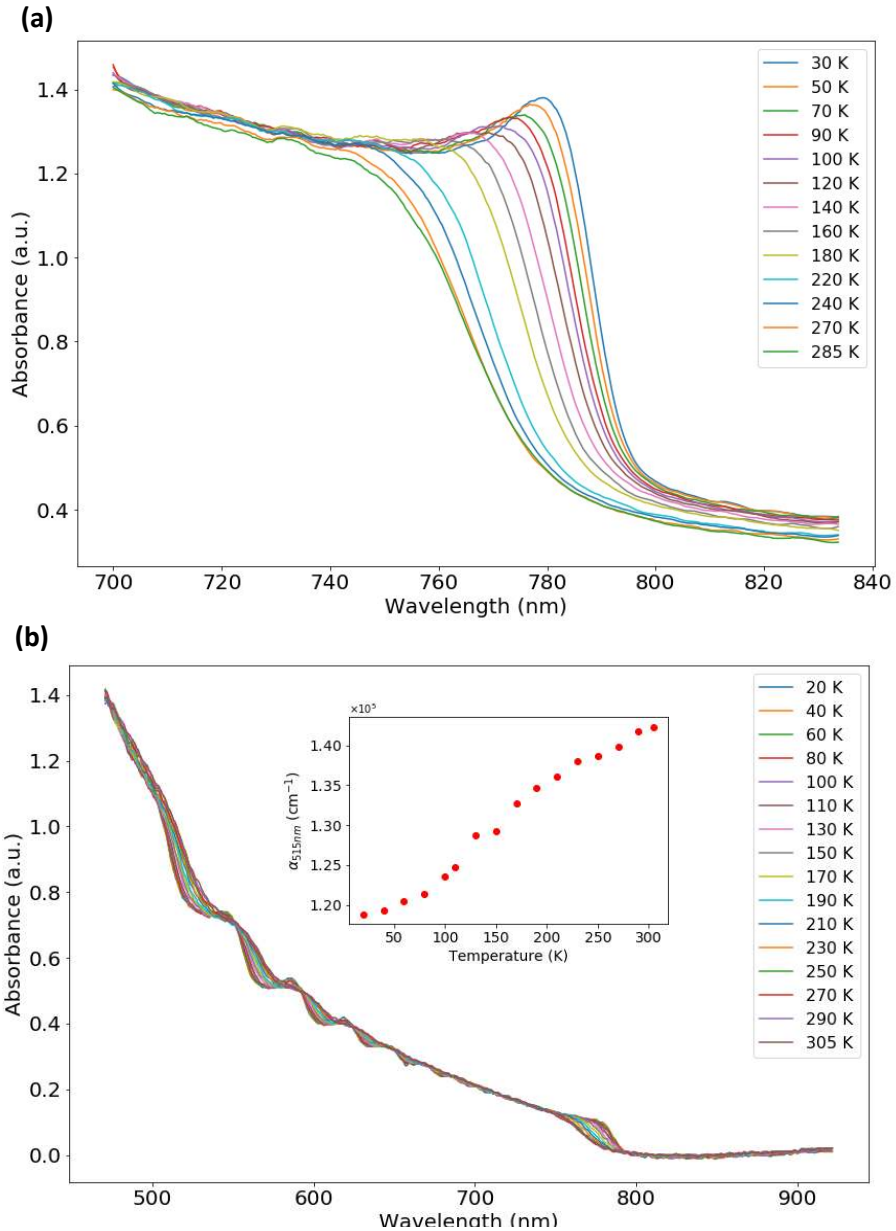

Figure S6: (a) Temperature-dependence of the absorbance spectra at selected temperatures on a film of thickness 769 nm, showing the emergence of an excitonic absorption peak upon cooling to around 150 K. **(b)** Temperature-dependence of the absorbance spectra at selected temperatures on a film of thickness 125 nm. *Inset:* temperature dependence of the absorption coefficient at λ = 515 nm.

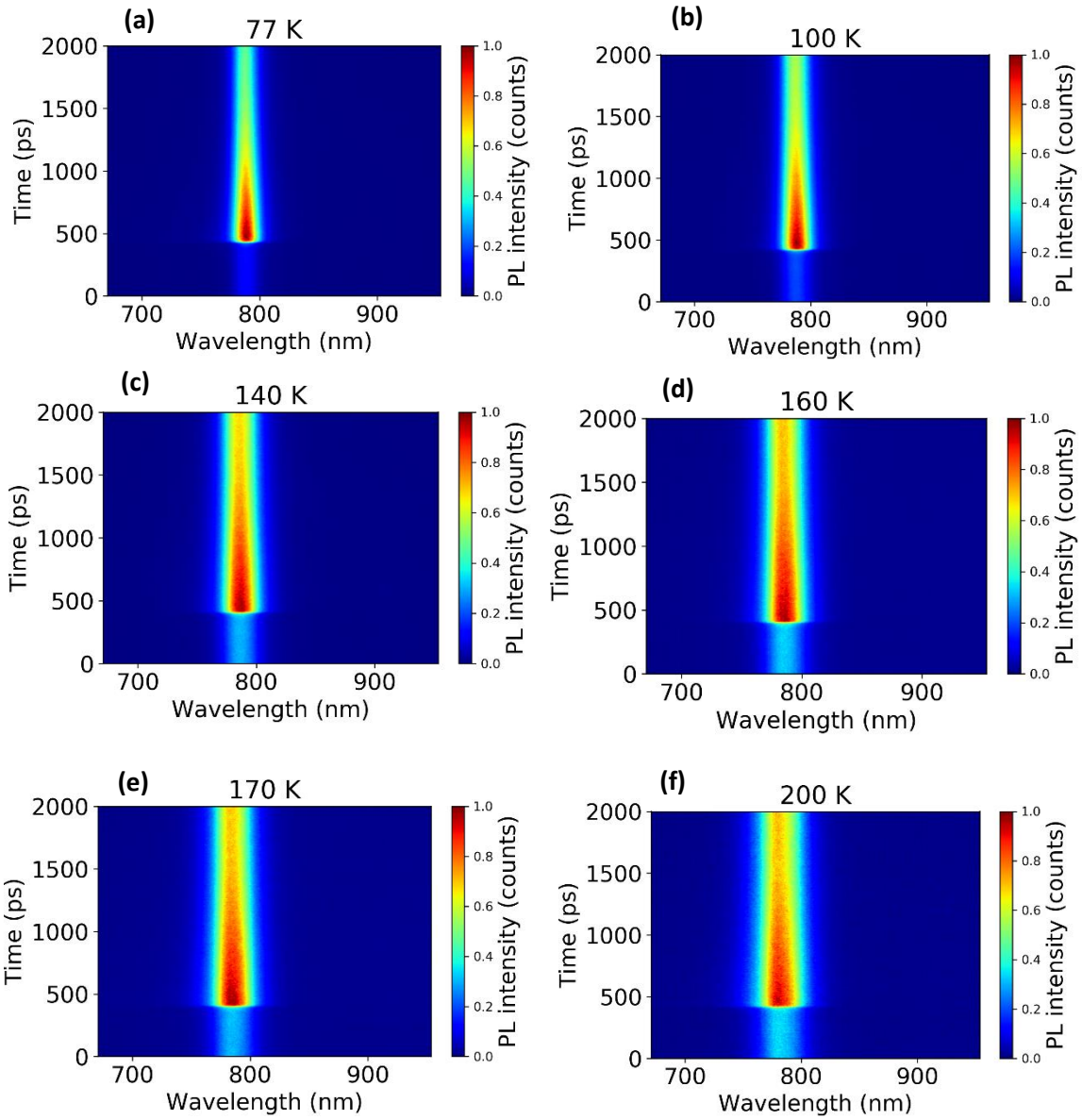

Figure S7(a-f): Temperature dependent time-resolved photoluminescence colormaps from streak camera data at a range of temperatures from **(a)** 77 K to **(f)** 200 K, at an excitation fluence of 3.1 μJcm^{-2}.

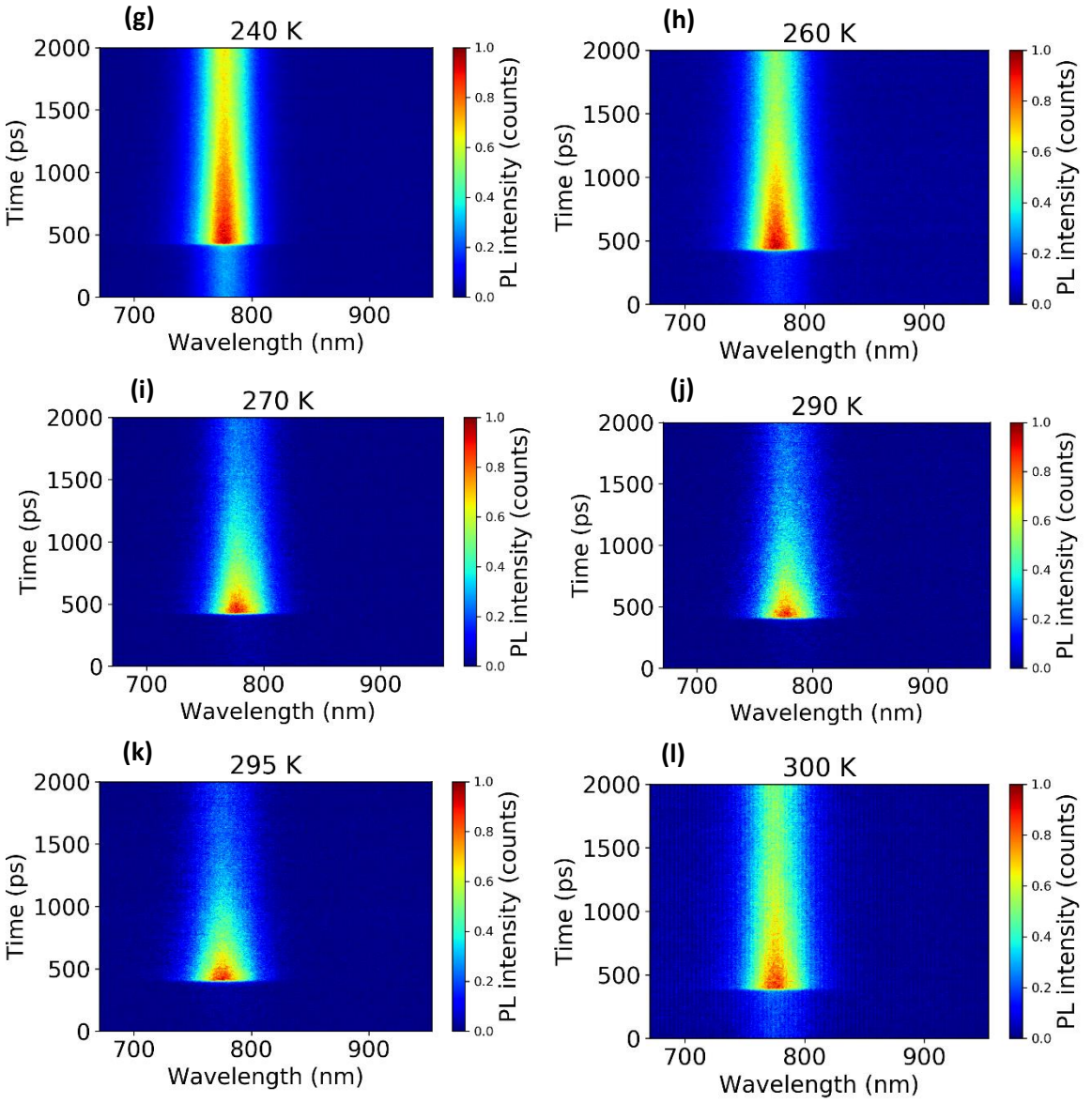

Figure S7(g-l): Temperature dependent time-resolved photoluminescence colormaps from streak camera data at a range of temperatures from **(g)** 240 K to **(l)** 300 K, at an excitation fluence of 3.1 μJcm^{-2}.

Supplementary Note 2: Temperature dependent PLQY

Temperature-dependent values of PLQY were calculated according to the following relation:

$$PLQY(T) = PLQY_{295K}\frac{PL(T)}{PL_{295K}}\frac{e^{-\alpha_{295K}L}}{e^{-\alpha(T)L}}$$

where $PLQY_{295K}$ is the value of PLQY as measured at 295 K (room temperature), PL_{295K} is the integrated photoluminescence at 295 K as determined from time-integrated PL measurements, $PL(T)$ is the integrated PL at temperature T. α_{295K} and $\alpha(T)$ are the absorption coefficients at 295 K and temperature T respectively, as determined from absorption measurements on $(FAPbI_3)_{0.85}(MAPbBr_3)_{0.15}$ thin films at the incident wavelength (λ = 515 nm).

The initial charge carrier density in the films was estimated using the following relation:

$$n_0\,(T) = \frac{E\,\lambda}{hc}\,\frac{(1 - e^{-\alpha(T)L})}{L}$$

where E is the excitation density of the incident laser light, λ is the laser wavelength, L is the average thickness of the film, and $\alpha(T)$ is the absorption coefficient in the material at temperature T. The factor $(1 - e^{-\alpha(T)L})$ accounts for the fraction of incident light absorbed by the film.

Alternate values of the initial charge carrier density were also estimated using:

$$n_0\,(T) = \frac{a(T)\,P}{E_{ph}\,f}\,\frac{1}{A\,L}$$

where $a(T)$ is the absorbance in the film at the excitation wavelength (λ = 515 nm) at temperature T, P is the laser power, E_{ph} is the energy of incident photons, f is the laser pulse frequency, A is the laser spot area and L is the average film thickness.[1]

Values of $n_0\,(T)$ were used to calculate approximate values for $k_2\,(T)$ from the radiative recombination rate $k_r(T)$ using the relation $k_2\,(T) \approx k_r(T)/n_0\,(T)$.

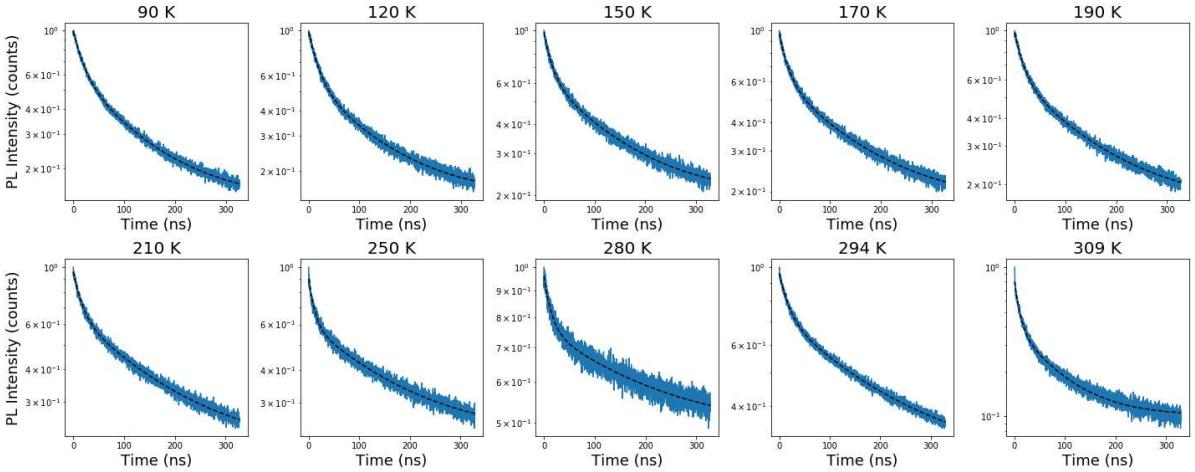

Figure S8: Examples of TRPL decay traces obtained from low fluence (approx. 30 nJ/cm^2) TCSPC measurements, from which approximate values of k_1 were determined by fitting the PL decay curve to a double exponential fit.

Supplementary Note 3: Low fluence TCSPC measurements

We can see from Figure S8 that, despite the low excitation fluence of approx. 30 nJ/cm^2, the TRPL decay traces are not monoexponential. This behaviour has been observed previously in low fluence TRPL measurements and has been attributed to localised recombination at grain boundaries and interfaces.[2] To obtain an estimate for k_1, we have therefore fitted the data with a double exponential of the form:

$$y(t) = A_1 e^{-\frac{t}{\tau_1}} + A_2 e^{-\frac{t}{\tau_2}}$$

where A_1 and A_2 are the amplitudes and τ_1 and τ_2 are the corresponding time constants of the fast and slow components of the decay, respectively. Values of these parameters for all temperatures are shown in Table S1. We took k_1 to be $1/\tau_2$, because it is the slow decay component τ_2 which describes the slow monomolecular behaviour associated with k_1. This allowed us to implement the fitting model based on a modified rate equation, as described in the main paper.

Temperature (K)	A_1	τ_1 (ns)	A_2	τ_2 (ns)
90	0.384	19.82	0.471	117.94
120	0.421	18.96	0.419	122.94
150	0.343	15.86	0.444	134.49
170	0.356	17.55	0.439	141.72
190	0.368	18.25	0.453	139.69
210	0.304	16.61	0.465	164.07
250	0.300	11.27	0.382	161.68
280	0.198	14.46	0.288	217.83
294	0.234	18.95	0.462	205.39
309	0.416	9.59	0.293	79.26

Table S1: Fitting parameters for a double exponential fit to low fluence (30 nJ/cm^2) TRPL data, at a series of temperatures from 90 K to 309 K.

References

[1] Richter *et al. Nat. Commun.* **2016**, *7*, 13941.

[2] D. W. de Quilettes *et al*. *Science* ***2015****, 348, 683.*